

MedChemComm

Accepted Manuscript



This is an *Accepted Manuscript*, which has been through the Royal Society of Chemistry peer review process and has been accepted for publication.

Accepted Manuscripts are published online shortly after acceptance, before technical editing, formatting and proof reading. Using this free service, authors can make their results available to the community, in citable form, before we publish the edited article. We will replace this *Accepted Manuscript* with the edited and formatted *Advance Article* as soon as it is available.

You can find more information about *Accepted Manuscripts* in the [Information for Authors](#).

Please note that technical editing may introduce minor changes to the text and/or graphics, which may alter content. The journal's standard [Terms & Conditions](#) and the [Ethical guidelines](#) still apply. In no event shall the Royal Society of Chemistry be held responsible for any errors or omissions in this *Accepted Manuscript* or any consequences arising from the use of any information it contains.

	Mukherjee, Kakoli; AstraZeneca India Pvt Ltd Hosagrahara, Vinayak; AstraZeneca India Pvt Ltd Solapure, Suresh ; AstraZeneca India Pvt Ltd Hameed P, Shahul; AstraZeneca India Pvt Ltd

SCHOLARONE™
Manuscripts



Scaffold Morphing Led to Evolution of 2,4-Diaminoquinolines and Aminopyrazolopyrimidines As Inhibitors of ATP Synthesis Pathway[†]

Received 00th January 20xx,
Accepted 00th January 20xx

DOI: 10.1039/x0xx00000x

www.rsc.org/

Subramanyam J. Tantry,^a Vikas Shinde,^a Gayathri Balakrishnan,^a Shankar D. Markad,^a Amit K. Gupta,^a Jyothi Bhat,^a Ashwini Narayan,^a Anandkumar Raichurkar,^a Lalit Kumar Jena,^a Sreevalli Sharma,^a Naveen Kumar,^a Robert Nanduri,^a Sowmya Bharath,^a Jitendar Reddy,^a Vijender Panduga,^a Prabhakar K. R.,^a Karthikeyan Kandaswamy,^a Parvinder Kaur,^a Neela Dinesh,^a Supreeth Guptha,^a Ramanatha Saralaya,^a Manoranjan Panda,^a Suresh Rudrapatna,^a Meenakshi Mallya,^a Harvey Rubin,^d Takahiro Yano,^d Khisi Mdluli,^b Christopher Cooper,^b V Balasubramanian,^a Vasan K. Sambandamurthy,^a Vasanthi Ramachandran,^a Radha Shandil,^a Stefan Kavanagh,^c Shridhar Narayanan,^a Pravin Iyer,^a Kakoli Mukherjee,^a Vinayak P Hosagrahara,^a Suresh Solapure,^a Shahul Hameed P,^{a*} Sudha Ravishankar.^{a*}

The success of bedaquiline as an anti-tubercular agent for the treatment of multi-drug resistant tuberculosis has validated ATP synthesis pathway and in particular ATP synthase as an attractive target. However, limitations associated with its use in the clinic and the drug-drug interactions with rifampicin have prompted research efforts towards identifying alternate ATP synthesis inhibitors with differentiated mechanism of action. A biochemical assay was employed to screen AstraZeneca's corporate compound collection to identify inhibitors of mycobacterial ATP synthesis. The high throughput screen resulted in the identification of 2, 4-diaminoquinazolines as inhibitors of ATP synthesis pathway. A structure activity relationship for quinazolines was established and the knowledge was utilized to morph quinazoline core into quinoline and pyrazolopyrimidine to expand the scope of chemical diversity. The morphed scaffolds exhibited a 10-fold improvement in the enzyme potency and over 100-fold improvement in selectivity against inhibition of mammalian mitochondrial ATP synthesis. These novel compounds were bactericidal and demonstrated growth retardation of *Mycobacterium tuberculosis* in the acute mouse model of tuberculosis infection.

^a Innovative Medicines, AstraZeneca India Pvt. Ltd., Bellary Road, Hebbal, Bangalore 560024, India.

^b Global Alliance for TB Drug Development, 40 Wall Street, 24th Floor, New York, NY 10005, USA.

^c AstraZeneca, Alderley Park, Mereside, Cheshire, UK.

^d University of Pennsylvania, 111 Clinical Research Building, 415 Curie Boulevard, Philadelphia PA 19104, USA

[†] The authors declare no competing interests.

Electronic Supplementary Information (ESI) available: [Materials and Methods; Synthesis schemes 1A and 1B; Fig. S1: 3D flexible superimposition of compound 3h, compound 8d and compound 17a with Bedaquiline, Figs. S2-S3: 2D binding site interaction of inhibitors - Bedaquiline, compound 3h, 8d, 12 and 17a at the ATPase binding site, Figs. S4-S7: NMR spectra and HPLC profiles of compounds 8g and 17a], associated with this article can be found in the online version. See DOI: 10.1039/x0xx00000x

1. Introduction

Tuberculosis (TB) caused by *Mycobacterium tuberculosis*, a highly infectious disease has plagued mankind for thousands of years. TB still remains a global pandemic causing around 1.4 million deaths and 9 million new incidences each year.¹ The financial burden of TB on developing countries is estimated to be between one and three trillion dollars over the next decade. Though the overall numbers of new cases have decreased by 40% since 1990, the global prevalence of multidrug resistant (MDR) and extensively drug resistant (XDR) TB has gone up substantially.²

TB can remain dormant for years after infection and can reactivate once the host become immunocompromised as in the case of HIV co-infected populations.³ Considerable progress has been made in TB drug discovery in the recent past and a number of drug candidates are at different stages of clinical trials.⁴ Diaryl quinoline (TMC207 or bedaquiline, **Fig. 1**), discovered by Johnson & Johnson pharmaceuticals and marketed as

SirturoTM, received expedited approval by the FDA for the treatment of MDR-TB.⁵ Thus a new TB drug with a different mode of action got approved after a gap of 40 years.^{5,6} Bedaquiline inhibits ATP synthase and causes depletion in intracellular ATP levels.⁷ This target is essential for the survival of bacteria under both replicating and non-replicating states, with a six times lower intracellular ATP levels during the non-replicating state as compared to the levels in the actively replicating state. Maintaining this threshold level of ATP is absolutely essential to keep the bacteria viable. Any further depletion would lead to a detrimental effect on bacterial survival.⁸ Although, ATP synthase is highly conserved and of fundamental importance to both prokaryotes and eukaryotes, bedaquiline is highly selective towards the mycobacterial enzyme. This critical information provides the rationale behind inhibiting a highly conserved target for clinical progression.⁹ The unprecedented success and novelty of bedaquiline has triggered several groups to investigate this pathway.

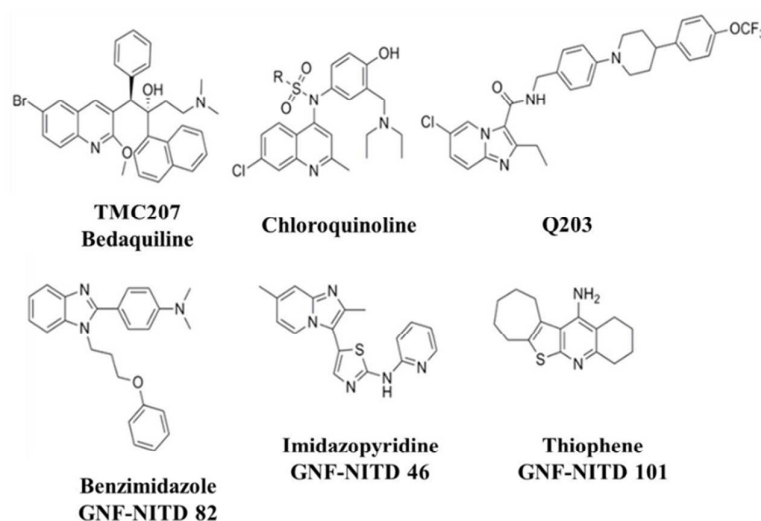


Fig. 1. Structures of ATP synthesis pathway inhibitors

Fig. 1 represents the structures of a few leading mycobacterial ATP synthase inhibitors reported in the literature to date.¹⁰⁻¹² In order to identify novel scaffolds targeting mycobacterial ATP-synthesis,

we screened AstraZeneca's corporate compound collection by employing a high throughput mycobacterial ATP synthesis assay (Myc_ATPS) which used *Mycobacterium smegmatis* membrane

preparation (inverted membrane vesicles - IMVs)¹³ to measure ATP synthesis via the oxidative phosphorylation (Ox-Phos) process. Compound **3a** (2, 4-diaminoquinazoline, **Fig. 2**) emerged as one of the promising hits from this high throughput screening (HTS) effort. However, this initial hit (**3a**) was not selective as it inhibited the mammalian mitochondrial ATP synthesis assay (SMP_ATPS) with equal potency. This report describes the results of medicinal chemistry structure activity relationship (SAR) efforts leading to the evolution of potent mycobacterial ATP synthesis pathway inhibitors, aminopyrazolopyrimidines and 2, 4-diaminoquinolines with about 20-fold and 120-fold selectivity window respectively.

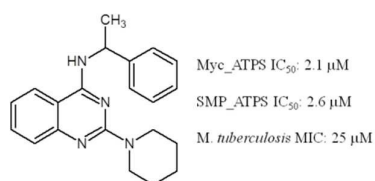


Fig. 2: Structure of HTS hit (compound **3a**)

2. Results and Discussion

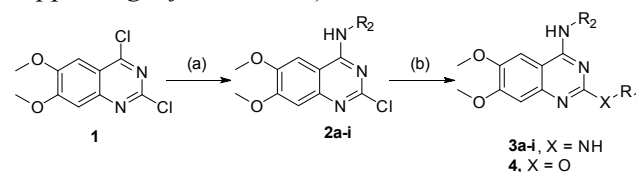
2.1. Chemistry

The syntheses of compounds derived from quinazoline, quinoline and pyrazolopyrimidine series are described in **schemes 1-4**.

2.1.1. Quinazoline derivatives (**3a-i**)

The required R₂ groups were incorporated by the displacement of 4-chloro functionality of 2,4-dichloro-6,7-dimethoxy-quinazoline with corresponding R₂-amines to give intermediates **2a-i** in good yields. Finally, 2-chloro of intermediates **2a-i** was displaced with R₁-amines under microwave conditions to provide compounds **3a-i** (**Scheme 1**). While most of the raw materials used as substitutions at R₁ and R₂ positions were procured commercially, one of the key intermediate 6-[2-(dimethylamino)ethoxy]-5-fluoropyridin-3-amine utilized for the synthesis of many of the

potent derivatives was obtained following a 4-step synthetic protocol starting from corresponding 3-fluoropyridin-2-ol (**Scheme 1A**, *supporting information 1*). Similarly, compound **4** with ether linkage at C2 position was synthesized by modification of the intermediate **2h** (**Scheme 1B**, *supporting information 1*)

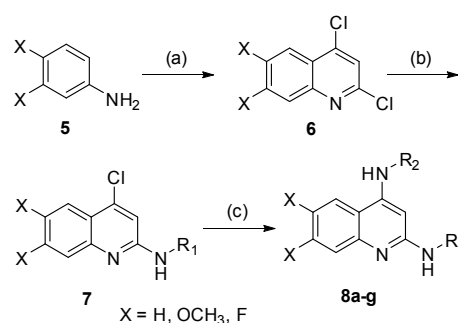


Scheme 1. Synthesis of 2, 4-diaminoquinolines.

Reagents and conditions: (a) R₂-NH₂, NaH, DMF, 80 °C, 2 h, yield: 45-55% and (b) R₁-NH₂, Na₂CO₃, *n*-BuOH, MW, 170 °C, 1.5 h, yield: 19-45%.

2.1.2. Quinoline derivatives (**8a-g**)

Condensation of malonic acid with aniline/substituted anilines **5** followed by treatment with POCl₃ gave substituted/unsubstituted 2,4-dichloroquinolines **6**. C₂-substitution with R₁-amines followed by C₄-substitution with R₂-amines under Buchwald-Hartwig reaction conditions gave compounds **8a-g** (**Scheme 2**).

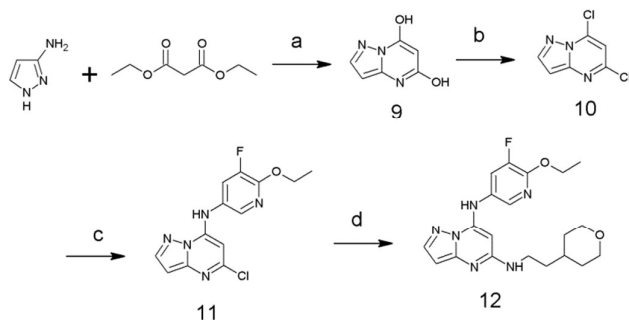


Scheme 2. Synthesis of 2, 4-diaminoquinolines.

Reagents and conditions: (a) Malonic acid, POCl₃, 120 °C, 6 h, yield: 60-65%; (b) Pd₂(dba)₃, XantPhos, NaOtBu, PhCH₃, 120 °C, MW 1 h, yield: 35-40%; (c) Pd₂(dba)₃, XantPhos, NaOtBu, PhCH₃, 120 °C, MW 1 h, yield: 7-72%.

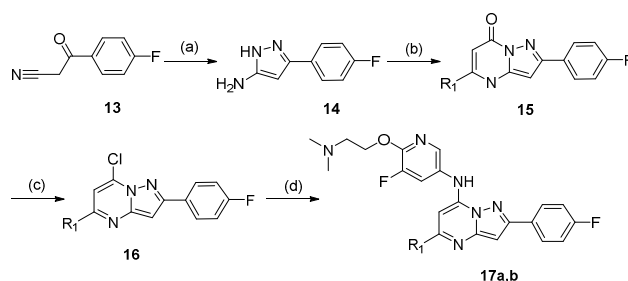
2.1.3. Pyrazolopyrimidine derivatives (**12**, **17a,b**)

Synthesis of compound **12** is described in **scheme 3a**. The condensation of diethyl malonate and 1H-pyrazol-3-amine with metallic sodium in ethanol resulted in cyclized 2,4-dihydroxy pyrazolopyrimidine intermediate **9**. Treatment of intermediate **9** with POCl₃ provided chloro intermediate **10**. Nucleophilic substitution of chloro intermediate **10** with 6-ethoxy-5-fluoropyridin-3-amine followed by a second nucleophilic substitution under microwave condition at C2 position resulted in compound **12**.



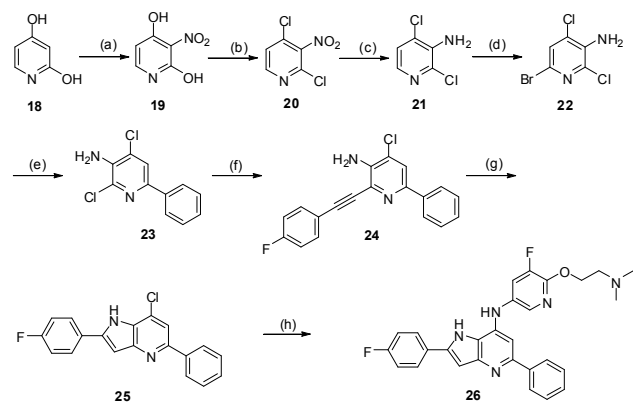
Scheme 3a. Synthesis of aminopyrazolopyrimidine 12. Reagents and conditions: (a) Na, EtOH, 85 °C, 18 h, yield: 62%; (b) POCl₃, 120 °C, 3 h, yield: 30%; (c) 6-ethoxy-5-fluoropyridin-3-amine, NaH, DMF, 75 °C, 2 h, yield: 94%; (d) 2-(tetrahydro-2H-pyran-4-yl) ethanamine, Na₂CO₃, DIPEA, n-BuOH, MW, 170 °C, 1.25 h, yield: 34%.

Synthesis of compounds **17a** and **17b** is described in **scheme 3b**. Condensation of 3-(4-fluorophenyl)-3-oxopropanenitrile **13** with hydrazine hydrate under heating conditions gave 5-aminopyrazole derivative **14**. The pyrazolopyrimidinone ring **15** was constructed by the reaction of 5-aminopyrazole derivative **14** with various R₁-substituted β-ketoesters. Treatment of compound **15** with POCl₃ provided chloro intermediate **16**. Nucleophilic substitution of chloro intermediate **16** with 6-[2-(dimethylamino)ethoxy]-5-fluoropyridin-3-amine (**Scheme 1A**, supporting information 1) afforded compounds **17a** and **17b** (**Scheme 3b**).



Scheme 3b. Synthesis of aminopyrazolopyrimidines. Reagents and conditions: (a) NH₂NH₂·H₂O, EtOH, 80 °C, 4 h, yield: 33%; (b) R₁-CO-CH₂-COOEt, AcOH, 120 °C, 12 h, yield: 48-55%; (c) POCl₃, 135 °C, 3 h, yield: 60-68%; (d) **1d**, K₂CO₃, DMF, 75 °C, 2 h, yield: 22-33%.

The synthesis of compound **26** with azaindole core is provided in **scheme 4**.



Scheme 4. Synthesis of azaindole 26. Reagents and conditions: (a) HNO₃, H₂SO₄, 0 °C, 0.5 h, yield: 85%; (b) POCl₃, 135 °C, 12 h, yield: 72%; (c) Fe, NH₄Cl, EtOH-H₂O, (4:1) 80 °C, 5 h, yield: 82%; (d) NBS, DMF, 0-25 °C, 1 h, yield: 47%; (e) PhB(OH)₂, Pd(PPh₃)₄, K₂CO₃, 1,4-dioxane, H₂O, 85 °C, 12 h, yield: 81%; (f) 1-ethynyl-4-fluorobenzene, Pd(Ph)₂Cl₂, CuI, TEA, 80 °C, 5 h, yield: 45%; (g) KO^tBu, THF, MW, 100 °C, 1 h, yield: 78%; (h) **1d**, ^tBuXPhos, THF, NaO^tBu, MW, 100 °C, 2 h, yield: 63%.

2.2. Structure Activity Relationship

The initial hit obtained from HTS campaign, compound **3a** (Fig. 2), was less potent in both enzyme assay (IC_{50} of 2.1 μ M) and anti-mycobacterial potency (*M. tuberculosis* minimum inhibitory concentration (MIC) of 25 μ M) as compared to some of the reported inhibitors of this pathway. Moreover, it had poor selectivity as it inhibited mammalian mitochondrial ATP synthesis (SMP_ATPS) with an IC_{50} of 2.6 μ M. The later assay was similar to Myc_ATPS assay in principle but used submitochondrial particles (SMP) from bovine heart mitochondria as the source of mitochondrial Ox-Phos components. Since ATP synthesis is a ubiquitous pathway and highly conserved across species, our initial efforts were focused on understanding the structure activity relationship (SAR) requirements of quinazoline series and improving the selectivity index (ratio of SMP_ATPS IC_{50} to Myc_ATPS IC_{50}). The molecular structure of compounds synthesized as part of this SAR effort along with their enzyme inhibitory and anti-mycobacterial potency have been listed in Table 1. Simple bioisosteric replacement of piperidine by pyrrolidine ring at C2 position tolerated for potency but the selectivity index got worsened for compound **3b** (Compound **3a** vs **3b**, Table 1). In the next round of design, we introduced polarity in the molecules at C2 and C4 position to improve selectivity and potency. Polarity modification hypothesis around compound **3a** resulted in achieving a 15-fold improvement in Myc_ATPS IC_{50} . Improved enzyme potency for compounds **3d**, **3e**, **3g** also translated into a 6 to 8-fold improvement in MIC but the selectivity index remained a concern for quinazoline series (Table 1) except for compounds **3d**, **3g** and **3i**.

Replacement of piperidine at the C2 position and α -methyl benzylamine at C4 position in compound **3b** with 2-(tetrahydro-2H-pyran-4-yl)ethanamine and 5-tert-butyl-1-methyl-1H-pyrazol-3-amine respectively yielded compound **3e** with no loss in potency suggesting that there is enough space for such hydrophobic groups. Introduction of additional polarity via dimethoxy

group at the C6, C7 positions of quinazoline ring resulted in a 10-fold improvement in enzyme potency and selectivity index for compound **3d** (Compound **3c** vs **3d**, Table 1). Later, we confined to having dimethoxy group substitution at C6, C7 during the majority of SAR modification due to potency gains observed and for reasons of ease of synthesis. Further replacement of pyrazole at C4 position by suitably substituted thiazole and pyridine ring systems tolerated for potency but the selectivity index was compromised by 5 fold (compound **3d** vs **3f**, Table 1). Substituting the pyran at C2 by pyridine ring system retained the enzyme potency with improved selectivity (compound **3f** vs **3g**, Table 1). However, the compound **3g** lost the MIC completely which may be due to bacterial permeability. Compound **4** with an ether linkage at C2 position was found to be inactive in both Myc_ATPS assay and *M. tuberculosis* MIC assay (Table 1). This indicated the requirement of an amino group at C2 position for mycobacterial ATP synthesis inhibition. The nitrogen here could be either secondary or tertiary and indicated that it is probably making a critical interaction with the enzyme. One of the explanations for this observed phenomenon could be the possible quaternization of nitrogen at physiological pH which is not possible with ether linkage. Elongation of ethoxy substitution of C4 pyridine side chain with terminal basic group showed moderate potency with enhanced selectivity index and an absolute IC_{50} of >25 μ M in SMP_ATPS assay (Compound **3h** vs **3i**, Table 1). This result suggested that an additional base centre in the molecule may provide handles for selectivity improvement without compromising on the potency.

None of the other attempts made to further resolve the issue around selectivity was successful for compounds with 2, 4-diaminoquinazoline core. Hence, we decided to expand the chemical scope of central core ring into 2, 4-diaminoquinoline and 5-phenylpyrazolo[1,5-a]pyrimidine. Majority of the SAR exploration on the new core was carried out

using 6-(2-(dimethylamino)ethoxy)-5-fluoropyridin-3-amine at R₁ position as this particular group on quinazoline, compound **3i**, had earlier resulted in an absolute IC₅₀ value of >25 μM against mammalian mitochondrial ATP synthesis.

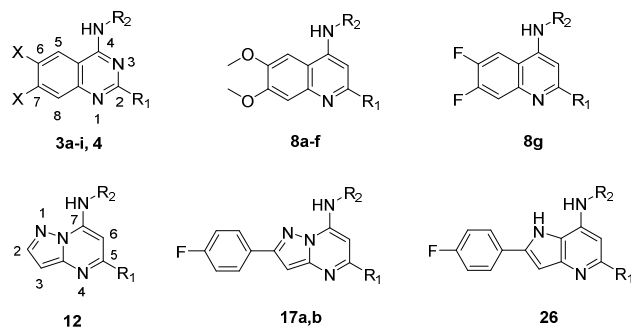


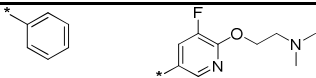
Fig. 3. Generic structures of synthesized compounds

Table 1: SAR around 2,4-diaminoquinazoline (**3a-3i**, **4**), 2,4-diaminoquinoline (**8a-8f**, **8g**) and aminopyrazolopyrimidine (**12**, **17a-17b**, **26**) cores.

CN. ^a	R ₁	R ₂	X	Myc_ATPS IC ₅₀ (μM)	M. tuberculosis MIC (μM)	Selectivity Index
3a			H	2.1	25	2.6
3b			H	2.5	50	<0.04
3c			H	1.7	6.2	4.5
3d			OCH ₃	0.1	6.2	52
3e			OCH ₃	0.1	6.2	ND ^b
3f			OCH ₃	0.4	3.1	10

Converting quinazoline core ring into quinoline by substituting N3 nitrogen with carbon weakened the enzyme potency marginally (Match pairs: **3h** vs **8a** and **3i** vs **8b** in **Table 1**). Encouraged with expanded chemical diversity of quinoline core with moderate enzyme potency, we then explored SAR of quinoline core with various R₁ substitutions to improve potency. Replacement of tetrahydropyranyl ethylamine substitution with 2-(2-chlorophenyl)ethanamine resulted in 60-fold improvement in enzyme potency and antimycobacterial activity (Match pair: Compound **8b** vs **8c**, **Table 1**). Compound **8c** also showed improved selectivity index (**Table 1**).

Journal Name	ARTICLE					
3g			OCH ₃	0.1	>200	96
3h			OCH ₃	0.6	1.9	2.3
3i			OCH ₃	0.9	25	>28
4			OCH ₃	25	>200	ND ^b
8a			-	0.8	6.2	3.2
8b			-	3.7	200	1
8c			-	0.06	3.1	79
8d			-	0.04	1.6	128
8e			-	0.06	6.2	44
8f			-	0.1	1.6	51
8g			-	0.1	3.1	19
12			-	21	>50	>1.2
17a			-	0.5	6.2	20
17b			-	0.5	12.5	19

26		-	0.1	0.8	13
----	-----------------------------------------------------------------------------------	---	-----	-----	----

^a Compound number, ^b not determined

The potency improvement observed with compound **8c** suggested that R₁ pocket may be hydrophobic in nature and the aromatic ring system would be a better alternative to an alicyclic ring in order to improve the potency. Further, conformational constraining of phenyl ethylamine group with 3-(2-chlorophenyl)pyrrolidine at R₂ position retained the potency and selectivity (Compound **8d** vs **8c**, Table 1). In a similar way, the conformational constraining of dimethylaminoethoxy group of R₁ substitution with N-methylpyrrolidine ring retained the enzyme potency but the selectivity index was compromised by 3-fold (Compound **8d** vs **8e**, Table 1). Replacement of oxygen linker of pyridine side chain with -NH linker in compound **8d** retained enzyme potency but anti-mycobacterial potency and selectivity were compromised by 2 to 3-fold (compound **8e** vs **8d**, Table 1). Modification of dimethoxy substitution of quinoline ring with difluoro group again retained potency but selectivity index was compromised by 6 to 7-fold. Overall, quinoline core demonstrated improved potency and selectivity compared to quinazoline core. Compound **8d** from quinoline series displayed the best IC₅₀, MIC, and selectivity index of 40 nM, 1.6 μM and 128-fold respectively (Table 1).

In an attempt to further expand chemical scope of the core ring system, we also morphed the central quinoline core to 5, 6-fused pyrazolopyrimidine ring system. The initial compound **12** was found to be inactive in both the biochemical and the anti-mycobacterial assay. In the absence of information on binding of these compounds at molecular level, we relied on chemical intuition to progress the series. Introduction of additional hydrophobic groups like fluorophenyl ring at the C2 position and a phenyl ring at the C5 position of pyrazolopyrimidine core

showed some promise of enzyme potency and *M. tuberculosis* MIC. Compound **17a** from pyrazolopyrimidine core demonstrated IC₅₀ and MIC of 0.5 μM and 6.2 μM respectively. Replacement of phenyl ring with suitable hydrophobic group like CF₃ at the C5 position of pyrazolopyrimidine (**17b**) core was found to be equipotent as that of **17a**. These results indicated that steric and/or hydrophobic factors could be mainly contributing to the potency rather than the planarity of phenyl ring (**17b** vs **17a**, Table 1). Further scaffold morphing was achieved by removing the bridge-head nitrogen of pyrazolopyrimidine and modifying central core into 4-azaindole ring system (Matched pair: **17a** vs **26**, Table 1). The resulting compound **26** showed best MIC in the series with *M. tuberculosis* MIC of 0.8 μM and Myc_ATPS IC₅₀ of 0.1 μM. Nevertheless, the selectivity index was compromised for compounds with pyrazolopyrimidine and azaindole cores compared to those with quinoline core. Among the different central core ring systems explored, compounds with quinoline core showed improved selectivity with compound **8d** demonstrating about 128-fold selectivity index, best among all the compounds synthesized. Fig. 3 provides a snapshot of the generic structures of the compounds synthesized in this study towards understanding the SAR.

2.3. Diaminoquinolines & aminopyrazolopyrimidines do not damage mycobacterial membrane

During the SAR exploration, compounds were tested for potency in the Myc_ATPS assay which used the inverted membrane vesicles prepared from *M. smegmatis* as source of Ox-Phos components. To ensure that the inhibition of ATP synthesis and the consequent *M. tuberculosis* MIC observed by

these compounds were not due to non-specific perturbation of the mycobacterial membrane, an assay was performed to test their potential to damage membrane and the results are given in **Table 2**. *M. bovis* Bacillus Calmette-Guerin (BCG) cells were used as surrogate in this membrane damage assay for reasons like its closeness to *M. tuberculosis* both at the genome and at the cellular architecture level, translation of *M. tuberculosis* MIC's in BCG and the ease of handling. This assay, an adaptation from the one reported for *S. aureus*, used a fluorophore, 3, 3'-Diethyloxycarbocyanine iodide (DiOC₂). A red shift in the emission wavelength is exhibited when DiOC₂ gets stacked in the bacterial cells.¹⁴

Table 2: Assessment of membrane damage potential

Compound	Myc_ATPS IC ₅₀ (μM)	BCG Membrane damage IC ₅₀ (μM)
3d	0.13	>100
8a	0.85	>100
8d	0.04	>100
8g	0.13	>100
17a	0.45	>100
17b	0.51	>100
26	0.13	>100
Bedaquiline	0.005	>100
CCCP	4.8	3

All compounds tested in this assay had an IC₅₀ of over 100 μM which is about hundred to thousand fold greater than the IC₅₀ in the Myc_ATPS assay suggesting that these compounds specifically inhibited mycobacterial ATP synthesis unlike the

positive control used in the assay, carbonyl cyanide m-chloro phenyl hydrazine (CCCP) had an IC₅₀ of 3 μM in the membrane damage assay while its IC₅₀ in the Myc_ATPS assay was also in the same range (**Table 2**).

2.4. Modeling studies with compounds 3h, 12 & 17a

Encouraged by the observation that the inhibition of ATP synthesis is not due to non-specific damage to the membrane, we utilized modeling studies to understand the possible interaction of these compounds with the ATP synthesis pathway component. The 2-dimensional (2D) tanimoto distance similarity (>50 %) as well as the 3-dimensional (3D) shape overlay similarity of select compounds **3h** (diaminoquinazoline core), **8d** (diaminoquinoline core) and **17a** (aminopyrazolopyrimidine core) with the crystal structure of bedaquiline led us to hypothesize that these inhibitors may occupy the binding cavity at the interface of the two c-subunits (chain B and chain C) and the a-subunit of ATP synthase similar to that reported for bedaquiline with *M. tuberculosis* ATP synthase (**Fig. S1, supporting information 2**).¹⁵ In order to predict the possible mode of binding and to understand the rationale observed from the structure activity relationship data in **Table 1**, we performed docking studies of these molecules at the active site using the earlier reported homology model of *M. tuberculosis* ATP synthase.¹⁶ Compounds were docked onto the bedaquiline binding site using Glide 6.1 extra precision(XP) method.¹⁷ The binding site interaction of bedaquiline in the *M. tuberculosis* ATP synthase model is shown in **Fig. 4**, where it bound the enzyme diagonally at the interface of the two c-subunits (chain B and chain C) and the a-subunit of ATP synthase. These interactions would plug the rotation of c-subunits resulting in the inhibition of ATP synthase and hence ATP synthesis (**Fig. 4A**).

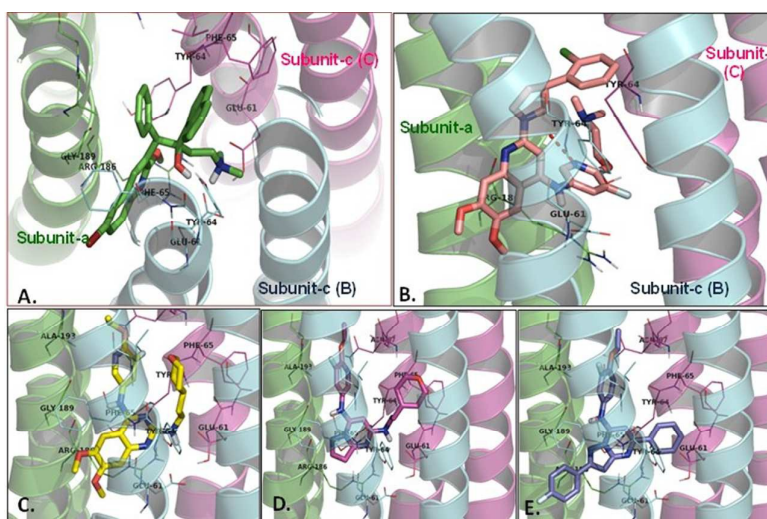


Fig. 4. Predicted binding mode of inhibitors. **A.** Bedaquiline (green colored carbon); **B.** Compound **8d** (amaranth pink colored carbon); **C.** Compound **3h** (yellow colored carbon) **D.** Compound **12** (pink colored carbon); **E.** Compound **17a** (blue colored carbon). Helices in cyan and pink color are chains A and B of c-subunit respectively whereas helix in green color is a-subunit of Fo component of ATP synthase.

The binding pose analysis of compound **8d** at the active site of *M. tuberculosis* ATP synthase revealed that dimethoxyquinoline group of **8d** interacts at the interface of Atp-a and Atp-c (chain-B) subunits through π - π interaction with Tyr-64 and H-bond interaction with Glu-61 and directs the fluoropyridin dimethoxyquinolin-4-amine group towards the interface of Atp-a and Atp-c (chain-C) subunits. Further, chlorophenyl group of the molecule nicely fitted into the hydrophobic cavity between the two Atp-c subunits (**Fig. 4B**). The occupancy of **8d** at the interface of Atp-a and Atp-c subunits caused the blockage of Atp-c subunit rotation and thereby its enzyme activity.

Similarly, the binding pose study of compound **3h** (**Fig. 4C**) revealed that the dimethoxy quinazoline group of **3h** occupied the cavity between Atp-a and Atp-c (chain-B) subunits. The amine group attached with pyridyl ring was found to interact with Arg-186 of Atp-a subunit, whereas the amine attached with pyran ring made H-bond contact with Glu-61 of Atp-c subunit (chain-B) providing strong anchorage to the molecule and place the pyran ring towards the hydrophobic space between the two Atp-c subunits.

The predicted binding mode of compound **12** (**Fig. 4D**) revealed the H-bond contact of pyrimidine nitrogen with Tyr-64 of Atp-c subunit (chain-B). The loss of Myc_ATPS inhibitory activity for compound **12** ($IC_{50} = 21 \mu M$) could be due to the lack of functional group to explore the hydrophobic pocket (constituting residues from Atp-a and Atp-c (chain-B) subunits) unlike bedaquiline where bromoquinoline exploits this region optimally (**Fig. 4C**). However, the pyran and pyridyl ring of the molecule showed similar binding pattern as noted for compound **3h**.

The binding pose comparison study of compound **17a** (**Fig. 4E**) showed that the addition of para fluoro phenyl group at pyrazole ring in compound **17a** allowed the compound to regain its interface blocking capacity between Atp-a and Atp-c (chain-B) subunits and hence regain the inhibitory potency. Further H-bond contact of pyrimidine nitrogen with Tyr-64 of Atp-c subunit (chain-B) anchored the ring and directed the attached phenyl ring to occupy the hydrophobic space between the two Atp-c subunits resulting in ATP synthase inhibitory activity of compound **17a** ($IC_{50} = 0.5 \mu M$) which is comparable to compound **3h**. Thus our docking study not only suggested the plausible

binding mode of these derivatives but also explained the activity variation among them.

2.5. Cross resistance profile of diaminoquinolines and aminopyrazolopyrimidines.

Computational studies led us to test diaminoquinoline and aminopyrazolopyrimidine derivatives against bedaquiline resistant mutants to check if they would exhibit the same mechanism of action as bedaquiline. A select set of compounds from these subseries were profiled against a panel of drug sensitive and drug resistant *M. tuberculosis* strains which included two of the bedaquiline resistant strains raised and characterized in-house. MICs against all the five drug sensitive and seven single drug resistant strains were the same as that of wild-type *M. tuberculosis* strain with no cross resistance observed in any of the mutants tested (Table 3). This data not only indicated that

diaminoquinoline and aminopyrazolopyrimidine compounds are equipotent against a range of drug sensitive *M. tuberculosis* strains but they are also equally active against several drug resistant strains satisfying one of the key requirements of a new TB drug candidate. However, the absence of cross resistance against bedaquiline resistant strains suggested that diaminoquinolines and aminopyrazolopyrimidines may not interact with ATP synthase in the same manner as bedaquiline despite binding at the same site. Thus, the key interactions to plug the rotation of the two c-subunits for diaminoquinoline and aminopyrazolopyrimidine derivatives could be different from the residues involved with the bedaquiline interaction. This needs to be further validated through characterization of mutants of *M. tuberculosis* resistant to diaminoquinoline and aminopyrazolopyrimidine derivatives.

Table 3: Cross resistance profile of diaminoquinolines and aminopyrazolopyrimidines

Inhibitor	MIC (μM)								
	Reference Sensitive strains		Single drug resistant strains					Reference lab strains	
	<i>M.tb</i> ATCC- 27294	<i>M.tb</i> strains*	<i>M.tb</i> 35820 STR ^R	<i>M.tb</i> 35822 INH ^R	<i>M.tb</i> 19000 RIF ^R	<i>M.tb</i> 17003 EMB ^R	<i>M.tb</i> 12119 OFX ^R	<i>M.tb</i> bedaquiline ^R (I66M)	<i>M.tb</i> bedaquiline ^R (A63P)
8d	6.3	3.1 - 12.5	12.5	6.3	3.1	6.3	12.5	6.3	3.1
8g	3.1	3.1 - 12.5	25.0	3.1	3.1	6.3	25.0	3.1	3.1
17a	6.3	6.3 - 12.5	25	12.5	6.3	6.3	12.5	6.3	12.5
26	3.1	3.1 - 6.3	25	3.1	3.1	6.3	25	3.1	3.1
Bedaquiline	0.2	<2	<2	<2	<2	<2	<2	10	>10
Streptomycin (STR)	0.3	0.3	> 11	0.3	0.3	0.3	0.3	0.3	0.3

ARTICLE									Journal Name
Isoniazid (INH)	0.2	0.2	0.2	>15	0.2	0.2	0.2	0.2	0.2
Rifampicin (RIF)	0.04	0.04	0.04	0.04	>1.2	0.04	0.04	0.04	0.04
Ethambutol (EMB)	9.8	9.8	9.8	9.8	9.8	>20	4.9	9.8	9.8
Ofloxacin (OFX)	0.7	0.7	0.7	0.7	0.7	0.3	>5.6	0.7	0.7

M.tb: M. tuberculosis

*MIC tested against four of *M. tuberculosis* drug sensitive strains: *M. tuberculosis* 25618, *M. tuberculosis*-Erdman, *M. tuberculosis*-Beijing (E-47/94), *M. tuberculosis*-Harlingen.

2.6. Diaminoquinolines & aminopyrazolo pyrimidines deplete intracellular ATP pool.

Inhibitors of ATP synthase enzyme or the other components of ATP synthesis pathway are expected to deplete the cells off their intracellular ATP pool. In order to test the ability of diaminoquinoline and aminopyrazolopyrimidine derivatives in reducing the intracellular ATP pool, we tested a representative set of compounds from these subseries in the intracellular ATP measurement assay. Cell lysates of BCG cultures which had been exposed to 5X MIC concentrations of these compounds for 20 hours were used to measure the intracellular ATP concentration. While isoniazid which inhibits FasII system showed no depletion in ATP levels, bedaquiline used as positive control exhibited 76% depletion in ATP levels. Compounds belonging to diaminoquinoline and aminopyrazolopyrimidines were not as potent as bedaquiline except for compound **8d** in reducing the cellular ATP levels suggesting a need to improve their potency further (Table 4).

Table 4: ATP pool depletion by diamino quinolines & aminopyrazolopyrimidines.

Inhibitor	% ATP depletion
INH	-6
Bedaquiline	76
8f	22
8g	25
8a	5
8d	68
17a	25

3h	31
26	23
None	0

2.7. Diaminoquinolines & aminopyrazolo pyrimidines are bactericidal but exhibit different kill rates

During the course of infection, *M. tuberculosis* is known to exist in various physiological states such as actively replicating and quiescent non-replicating forms. Inhibitors of the energy production pathway are known to make the pathogen highly vulnerable resulting in bactericidal effect.^{7,18} A select set of compounds from the subseries were tested for their growth inhibitory properties under aerobic and hypoxic conditions (used as a model for non-replicating bacilli). All the compounds tested were bactericidal under both aerobic and hypoxic conditions with a minimum bactericidal concentration (MBC) to MIC ratio reaching a maximum of 15 except for compound **8d** (Table 5). However, the two scaffolds differed in kill rates as determined by the *in vitro* kill kinetics under replicating conditions. Compound **8g** (diaminoquinoline) showed a faster kill rate, dependent on both concentration and time whereas **17a** (aminopyrazolopyrimidine) seemed to display a dependence on time for cidalty (Figs. 5A and 5B).

Table 5: Bactericidal activity of diamino quinolines & aminopyrazolopyrimidines

Compound	Aerobic		Hypoxic
	<i>M.tb</i> MIC (μM)	<i>M.tb</i> MBC (μM)	<i>M.tb</i> MBC (μM)
3d	6.2	25	50
3f	3.1	25	13
3h	2.2	19	3
3e	6.2	25	50
8d	2.2	54	200
8g	3.1	38	50
8e	6.2	50	50
17a	7.4	28	100
Bedaquiline	0.2	1.6	4

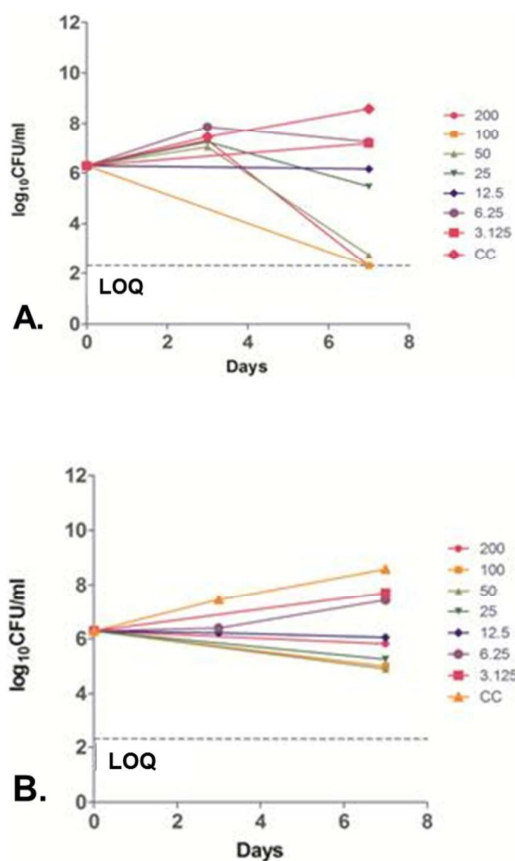
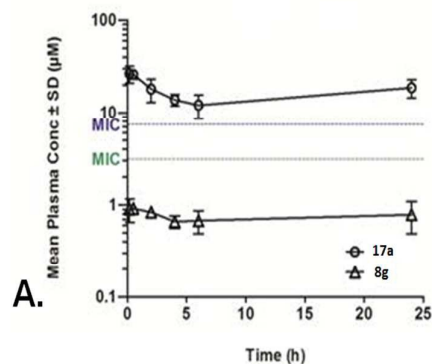


Fig. 5. *In vitro* survival kinetics of 8g and 17a: *M. tuberculosis* cells were exposed to 0–200 μM of compounds **8g** (A) and **17a** (B) over a period of 7 days. Appropriate dilutions of culture samples were plated for measuring colony forming units on 7H11 plates on 0 (start of exposure), 3 and 7 days post compound exposure.

2.8. Diaminoquinolines & amino pyrazolo pyrimidines retard growth of *M. tuberculosis* in a mouse model of TB infection

Based on the potency and selectivity for inhibition of mycobacterial ATP synthesis, **17a** and **8g** were tested for efficacy in an acute model of TB infection. Plasma concentration-time profiles in infected mice have been shown in Fig. 6A. In the infected mice, total plasma concentration of **17a** was above MIC for 24 h whereas the same for **8g** was below MIC during the entire dosing interval. Both the compounds were able to retard the growth of *M. tuberculosis* during the course of infection in mouse lungs unlike the reference drug isoniazid which exhibited a bactericidal effect by reducing the bacterial load by more than two logs in the two week treatment period (Fig. 6B).



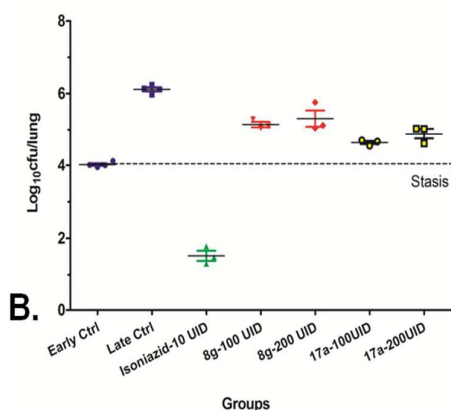


Fig. 6. (A) Pharmacokinetic profiles - 8g and 17a were orally administered as a suspension in 0.5% hydroxypropyl methylcellulose (HPMC) & Tween 80 at a 10-ml/kg dose volume and **(B) Log₁₀ lung CFU** in various groups: untreated early control (blue circles, filled) after 3 days of infection; untreated late control (blue squares, filled) after 2 weeks of infection; after treatment with isoniazid at 10 mg/kg (green symbols) or with **8g** (red symbols) or **17a** (yellow symbols) at 100 or 200 mg/kg once daily (UID), 6 days per week for 2 weeks.

Growth retardation effect by compound **17a** was more pronounced than that of **8g** probably due to its higher plasma concentration. However, the extent of growth inhibition observed with both compounds seemed to be maximal as no dose response effect was seen with the two doses (100 and 200 mg/kg) tested in the study. The growth inhibition observed with **8g** despite its lower plasma concentration could be due to the accumulation of the compounds in the mouse lungs.

Conclusion

In conclusion, we report here the discovery of diaminoquinoline, aminopyrazolopyrimidines and azaindoles as novel mycobacterial ATP synthesis inhibitors with potent *M. tuberculosis* MIC. Like bedaquiline, these compounds were found to

inhibit *M. tuberculosis* growth by reducing the intracellular ATP pool although not as effectively as bedaquiline. Docking studies implicated the mode of action to be the inhibition of ATP synthase enzyme, however, the exact molecular mechanism of how these compounds deplete the cells off ATP still needs to be elucidated as no cross resistance was observed with bedaquiline resistant mutants. Scaffold morphing efforts resulted in the identification of multiple cores which enhanced the scope of SAR expansion for the series. Compounds belonging to diaminoquinoline subseries exhibited best enzyme inhibition and anti-mycobacterial potency with a fairly good selectivity index among all the compounds analyzed. Representative compounds from the all subseries exhibited bactericidal activity against *M. tuberculosis* and were able to demonstrate growth retardation of the bacilli in the lungs of infected mice as compared to the uninhibited control in a murine model of tuberculosis infection.

Additional medicinal chemistry efforts are needed to further optimize the potency, selectivity and pharmacokinetic profiles of these lead series to identify a clinical candidate. Being a novel chemotype with activity against bedaquiline resistant mutant, we believe that this class of compounds has the potential to be developed as an anti-TB drug candidate.

Abbreviations

M.tb: *M. tuberculosis*

Ox-Phos: Oxidative phosphorylation

DiOC2: Diethyloxacarbocyanine iodide

CCCP: Carbonyl cyanide m-chloro phenyl hydrazine

Myc_ATPS: Mycobacterial ATP synthesis assay

SMP_ATPS: Mitochondrial ATP synthesis assay

MIC: Minimum Inhibitory Concentration

MBC: Minimum Bactericidal Concentration

Author Contributions

S.J.T., S.H.P, S.D.M., A.R., C.C., P.I. and M.P. are responsible for medicinal chemistry design and analyses. S.J.T., V.S., S.D.M. and L.K.J. are responsible for synthetic chemistry. S.R. and M.M are responsible for compound purity. A.K.G and M.P. designed and performed the modelling. S.H.P., K.M., M.P., S.K. M.M. and V.B. performed the hit triage for the high through screen output. K.M., H.R., T.Y. and K.M. designed IC₅₀ determination experiments. G.B. and J.B. performed IC₅₀ determination experiments and analyzed the data. V.R., V.K.S., K.M., V.B. and S.R. designed the microbiology experiments. A.N., S.S., P.K., N.D., S.G., performed microbiology experiments. V.P.H., S.S., S.N. and R.S. Designed and Analyzed PK-PD experiments. N.K., R.N., S.B., J.R., V.P., P.K.R., K.K. and R.S. performed PK-PD experiments. S.R., G.B. and J.B designed, performed and analyzed ATP pool measurement assay. S.J.T., S.D.M., A.K.G., S.R. and S.H.P wrote the manuscript with contributions from all co-authors.

Acknowledgment

We sincerely thank the compound management group (AstraZeneca Bangalore), DMPK (AstraZeneca, Waltham, USA), and Global Discovery Sciences, Global Safety Assessment (AstraZeneca, Alderley Park, UK) for technical support. We thank Ms. Anisha Ambady and Ms. Naina V Mudugal for providing the Bedaquiline resistant mutants. We acknowledge Sandeep Ghorpade and Pravin Shirude for scientific discussions. We also thank Dr. R. Tommasi and Dr. T. S. Balganesesh for their constant support and encouragement.

Funding Sources

Global Alliance for TB Drug Development.

References

1. The TB pandemic, <http://www.tballiance.org/why/the-tb-pandemic.php>
2. World Health Organization, World TB day **2013** report, <http://www.who.int/campaigns/tb-day/2013/event/en/>
3. Pawlowski A, Jansson M, Skold M, Rottenberg ME, Kallenius G. Tuberculosis and HIV Co-Infection. *PLoS pathog.* **2012**, 8, 1.
4. Zumla A, Nahid P, Cole ST. Advances in the development of new tuberculosis drugs and treatment regimens. *Nature* **2013**, 12, 388.
5. Cohen J. Approval of novel TB drug celebrated with restraint. *Science* **2013**, 339, 130.
6. Mahajan R. Bedaquiline: First FDA-approved tuberculosis drug in 40 years. *Int. J. Appl. Basic Med. Res.* **2013**, 3, 1.
7. Andries K, Verhasselt P, Guillemont JEG, Gohlmann HWH, Neefs JM, Winkler H, van Gestel J, Timmerman P, Zhu M, Lee E, Williams P, de Chaffoy D, Huitric E, Hoffner SE, Cambau E, Truffot-Pernot C, Lounis N, Jarlier VA. A diarylquinoline drug active on the ATP synthase of *Mycobacterium tuberculosis*. *Science* **2005**, 307, 223.
8. Gengenbacher M, Rao SP, Pethe K, Dick T. Nutrient-starved, non-replicating *Mycobacterium tuberculosis* requires respiration, ATP synthase and isocitrate lyase for maintenance of ATP homeostasis and viability. *Microbiology* **2010**, 156, 81.
9. Haagsma AC, Abdillahi-Ibrahim R, Wagner MJ, Krab K, Vergauwen K, Guillemont J, Andries K, Lill H, Koul A, Bald D. Selectivity of TMC207 towards mycobacterial ATP synthase compared with that towards the eukaryotic homologue. *Antimicrob. Agents Chemother.* **2009**, 53, 1290.
10. Khan SR, Singh S, Roy KK, Akhtar MS, Saxena AK, Krishnan MY. Biological evaluation of novel substituted chloroquinolines targeting mycobacterial ATP synthase. *Int. J. Antimicrobial Agents.* **2013**, 41, 41.
11. Pethe K, Bifan P, Jang J, Kang S, Park S, Ahn S, Jiricek J, Jung J, Jeon HK, Cechetto J, Christophe T, Lee H, Kemp M, Jackson M, Lenaerts AJ, Pham H, Jones V, Seo MJ, Kim YM, Seo M, Seo JJ, Park D, Ko Y, Cho I, Kim R, Kim SY, Lim SB, Yim S, Nam J, Kang H, Kwon H, Oh C, Cho Y, Jang Y, Kim J, Chua A, Tan B, Nanjundappa MB, Rao SPS, Barnes WS, Wintjens R, Walker JR, Alonso S, Lee S, Kim J, Oh S, Oh T, Nehrbass U, Han SJ, No Z, Lee J, Brodin P, Cho SN, Nam K, Kim J. Discovery of Q203, a potent clinical candidate for the treatment of tuberculosis. *J. Nat. Med.* **2013**, 19, 1157.
12. Mak PA, Rao SPS, Tan MP, Lin X, Chyba J, Tay J, Hwee Ng S, Tan BH, Cheri-an J, Duraiswamy J, Bifani P, Lim V, Lee BH, Ma NL, Beer D, Thayalan P, Kuhen K, Chatterjee A, Supek F, Glynne R, Zheng J, Boshoff HI, Barry 3rd CE, Dick T, Pethe K, Camacho LR. A high-throughput screen to identify inhibitors of ATP homeostasis in non-replicating *Mycobacterium tuberculosis*. *ACS Chem. Biol.* **2012**, 7, 1190.
13. Yano T, Kassovska-Bratinova S, Teh JS, Winkler J, Sullivan K, Issacs A, Schechter NM, Rubin H. Reduction of clofazimine by mycobacterial type 2 NADH:Quinine Oxidoreductase. *J. Biol. Chem.* **2011**, 25, 10276.
14. Gentry DR, Wilding I, Johnson JM, Chen D, Remlinger K, Richards C, Neill S, Zalacain Rittenhouse SF, Gwynn MN. A rapid microtiter plate assay for measuring the effect of compounds on *Staphylococcus aureus* membrane potential. *J. Microbiol. Meth.* **2010**, 83, 254.
15. Segala E, Sougakoff W, Nevejans-Chauffour A, Jarlier V, Petrella S. New mutations in the mycobacterial ATP synthase: new insights into the binding of the diarylquinoline TMC207 to the ATP synthase C-ring structure. *Antimicrob. Agents Chemother.* **2012**, 56, 2326.

18

16. de Jonge MR, Koymans LH, Guillemont JE, Koul A, Andries K. A computational model of the inhibition of *Mycobacterium tuberculosis* ATPase by a new drug candidate R207910. *Proteins*. **2007**, 67, 971.
17. Glide version 6.1, Schrodinger, LLC, NY, **2013**.
18. Rao SPS, Alonso S, Rand L, Dick T, Pethe K. A proton motive force is required for maintaining ATP homeostasis and viability of hypoxic, non-replicating *Mycobacterium tuberculosis*. *Proc. Natl. Acad. Sci.* **2008**, 105, 11945.

Scaffold Morphing Led to Evolution of 2, 4-Diaminoquinolines and Aminopyrazolopyrimidines as Inhibitors of ATP Synthesis Pathway

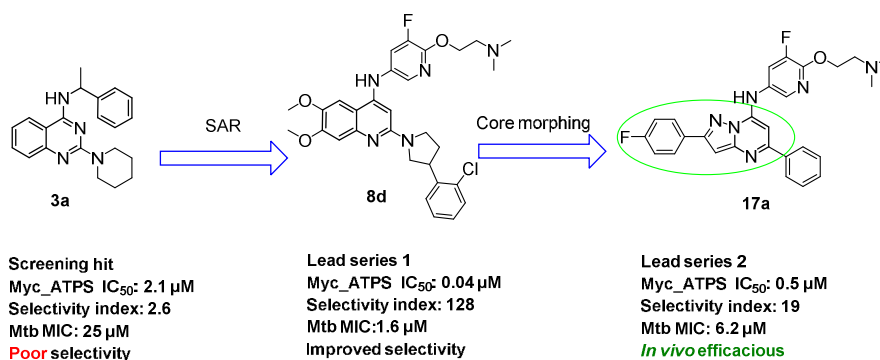
Subramanyam J. Tantry,^a Vikas Shinde,^a Gayathri Balakrishnan,^a Shankar D. Markad,^a Amit K Gupta,^a Jyothi Bhat,^a Ashwini Narayan,^a Anandkumar Raichurkar,^a Lalit Kumar Jena,^a Sreevalli Sharma,^a Naveen Kumar,^a Robert Nanduri,^a Sowmya Bharath,^a Jitendar Reddy,^a Vijender Panduga,^a Prabhakar K. R,^a Karthikeyan Kandaswamy,^a Parvinder Kaur,^a Neela Dinesh,^a Supreeth Guptha,^a Ramanatha Saralaya,^a Manoranjan Panda,^a Suresh Rudrapatna,^a Meenakshi Mallya,^a Harvey Rubin,^d Takahiro Yano,^d Khisi Mdluli,^b Christopher Cooper,^b Balasubramanian V,^a Vasan K. Sambandamurthy,^a Vasanthi Ramachandran,^a Radha Shandil,^a Stefan Kavanagh,^c Shridhar Narayanan,^a Pravin Iyer,^a Kakoli Mukherjee,^a Vinayak P Hosagrahara,^a Suresh Solapure,^a Shahul Hameed P,^{a*} Sudha Ravishankar.^{a*}

^a Innovative Medicines, AstraZeneca India Pvt. Ltd., Bellary Road, Hebbal, Bangalore 560024, India.

^b Global Alliance for TB Drug Development, 40 Wall Street, 24th Floor. New York, NY 10005, USA.

^c AstraZeneca, Alderley Park, Mereside, Cheshire, UK.

^d University of Pennsylvania, 111 Clinical Research Building, 415 Curie Boulevard, Philadelphia PA 19104, USA



2, 4-diaminoquinazolines, 2, 4-diaminoquinolines and aminopyrazolopyrimidines, inhibitors of mycobacterial ATP synthesis, are novel lead molecules towards discovery and development of new anti-tubercular agents.